Sizing and Optimization
of the Horizontal Tail of a Jet Trainer

Sinem Karatoprak* and Prof. Dr. Serkan Özgen**
* *Flight Mechanics Dept., Aircraft Group, Turkish Aerospace Inc. (TA), Ankara 06980, Turkey*
** *Dept. Aerospace Engineering, Middle East Technical University (METU), Ankara 06800, Turkey*

Abstract

The size of horizontal tail is determined to meet stability and control requirements over the specified center-of-gravity range for a conventional jet trainer aircraft. Aircraft had to have inherent longitudinal stability throughout the flight envelope until the early 1970s. However, the concept of relaxed static stability (RSS) arose with the advent of active control technology (ACT). ACT allows aircraft to fly operationally with negative inherent airframe stability, that has the advantages of smaller tail volume, hence less weight. In this paper, tail sizing diagrams are created to find the minimum required horizontal tail size over a required CG range for both conventional aircraft and aircraft with RSS.

1. Introduction

The horizontal tail of an aircraft is required to provide necessary longitudinal control and the sufficient static stability throughout the defined center-of-gravity (CG) range. Therefore, the horizontal tail must be sized in accordance with these considerations.

The required horizontal tail area at forward (FWD) CG limit is typically set by the control authority to lift the nosewheel on take-off, while the aft center-of-gravity limit requirement is typically determined by the minimum sufficient static longitudinal stability and high angle of attack nose down recovery.

The horizontal tail provides enough static stability in pitch up to the most aft center-of-gravity position. Stability is really essential for an aircraft during flight since a nose-up disturbance aggravates nose-up tendency in an unstable case. In order to determine whether an aircraft is stable, the determination of the static margin (SM) is one of the methods. For a conventional aircraft, static margin is approximately minimum positive 5 - 3 % in the subsonic flight regime. However, a large backward aerodynamic center (AC) shift occurs between subsonic to supersonic transition. This causes a large increase in static margin at supersonic flight regime, which penalizes the performance in terms of drag (mostly trim drag) and weight. The concept of RSS arises due to this shift in aerodynamic center. The essence of RSS is that the size of the horizontal tail is reduced. The aircraft operates with negative static margins at subsonic speeds in order to reduce the large static margins in supersonic flight regime. The result is a reduction in gross weight, a reduction in trim drag, and an improvement in maneuverability.

The horizontal tail also supplies adequate control throughout the defined center-of-gravity range during takeoff and landing. The horizontal tail must have enough control authority to rotate the aircraft nose-up about its main landing gear during takeoff and to trim aircraft during approach. The controllability of the aircraft must be kept even after the inherent stability is relaxed.

In the scope of this study, the effect of horizontal tail area on longitudinal stability and control is investigated. Therefore, several horizontal tails with different planform areas were analyzed with Computational Fluid Dynamics (CFD) and DATCOM [8].

Tail sizing diagrams known as an x-plots or scissor-plots for all of the horizontal tails are created to find the minimum required horizontal tail size over the defined center-of-gravity range. These diagrams show the forward and aft center-of-gravity limits against the non-dimensional horizontal tail volume. The minimum size of the horizontal tail size is determined throughout the required CG range by being choosing the smallest tail volume coefficient.

Sinem Karatoprak, Serkan Özgen

2. Nomenclature

AC	: aerodynamic center
ACT	: active control technology
AoA	: angle of attack
AoS	: angle of sideslip
AR	: aspect ratio
b	: wing span
b_{HT}	: horizontal tail span
$\bar{c}$	: mean wing aerodynamic chord
CFD	: computational fluid dynamics
CG	: center-of-gravity
C_{HT}	: horizontal tail volume coefficient
$\bar{c}_{HT}$	: mean horizontal tail aerodynamic chord
C_L	: lift coefficient
C_m	: pitch moment coefficient
$C_{m_{ac}}$	: pitch moment coefficient about wing aerodynamic center
D	: aircraft drag
FWD	: forward
HT	: horizontal tail
l_{HT}	: distance from center-of-gravity to quarter-chord of the horizontal tail
L	: total lift
L_h	: tail lift
L_{wf}	: wing-fuselage lift
M_{CG}	: pitch moment about center-of-gravity
MAC	: mean aerodynamic chord
NP	: neutral point
$\bar{q}$	: dynamic pressure
$\dot{q}$	: pitch angular acceleration
R	: reaction force
RSS	: relaxed static stability
S	: wing reference area
S_{HT}	: horizontal tail area
S_{ref}	: wing reference area
T	: thrust
W	: aircraft weight
X_{AC}	: location of wing aerodynamic center
X_{AC_h}	: location of horizontal tail aerodynamic center
X_{cg}	: location of center-of-gravity
X_{mg}	: distance defined in *Figure 6*
X_{NP}	: location of neutral point
Z_{cg}	: distance defined in *Figure 6*
Z_D	: distance defined in *Figure 6*
Z_{mg}	: distance defined in *Figure 6*
Z_T	: distance defined in *Figure 6*
α	: angle of attack
Λ_{LE}	: leading edge sweep angle
μ	: friction coefficient
$\ddot{\theta}_{mg}$	: angular acceleration about main landing gear

3. Aircraft Specifications and Analyzed Configurations & Conditions

3.1. Aircraft Specifications

The major parameters of the jet trainer used during this study are tabulated in Table 1.

Table 1: Major Aircraft Specifications

Aircraft Specifications			
$\bar{c}$ (m)	2.70 m	T (N)	69677
S (m^2)	24 m^2	Z_{cg}(m)	2.10
I$_{YY}$ (kg.m^2)	46162	Z_D (m)	1.82
X_{mg} (m)	8.16	Z_{mg}(m)	0
$X_{AC_{wf}}$ (m)	7.62	Z_T(m)	1.85
Forward CG (% of mac)	35	X_{AC_h} (m)	11.85
Aft CG (% of mac)	39		

3.2. Analyzed Configurations

The analyses were conducted for six different horizontal tail areas. Parameters such as aspect ratio, sweep angle, taper ratio, etc. remain same during the analyses. The detailed information about parameters of horizontal tails are given in Table 2.

Table 2: Planform Parameters of Six Horizontal Tail

Horizontal Tail Parameters	HT#1	HT#2	HT#3	HT#4	HT#5	HT#6
b_{HT} (m)	5.041	5.226	5.578	5.91	6.223	6.521
$\bar{c}_{HT}$ (m)	1.592	1.651	1.762	1.87	1.966	2.060
S_{HT} (m^2)	7.261	7.804	8.891	9.98	11.064	12.151
AR	3.5	3.5	3.5	3.5	3.5	3.5
Λ_{LE} (°)	37	37	37	37	37	37
C$_{HT}$	0.468	0.503	0.573	0.64	0.713	0.783

3.3. Analyzed Conditions

The analyzed conditions are determined by considering the type of maneuver to avoid unnecessary analysis points.

The longitudinal static stability and nose-down recovery characteristics are evaluated for subsonic, transonic and supersonic speeds, while the take-off rotation is evaluated naturally for low subsonic speed. The analyzed conditions are tabulated in Table 3.

Table 3: The Analysis Conditions

The Analysis Parameters	Longitudinal Static Stability	Nose-Down Recovery	Take-Off Rotation
Flap deflection	Non-Deflected	Non-Deflected	25
HT deflection (°)	Non-Deflected	+30	-30
Speed (Mach)	0.2, 0.9, 1.2	0.2, 0.9, 1.2	0.2
AoA (°)	0, 3, 9, 15, 20, 25	15 (for 1.2 Mach) 25 (for 0.2 and 0.9 Mach)	0
AoS (°)	0	0	0

4. Horizontal Tail Sizing Requirements

The horizontal tail is sized to ensure a sufficient level of static stability and the required longitudinal control in a conventional aircraft design. The size of horizontal tail is determined by the following three primary requirements, which are defined in detail below:

- The longitudinal static stability of the aircraft at the aft CG position,
- The nose-down control authority for recovery at high AoA and aft CG position,
- The control authority of horizontal tail during take-off rotation at forward CG position.

4.1 Longitudinal Static Stability

Static equilibrium means that there is no linear or rotational acceleration of the aircraft. The sum of forces and moments acting on the aircraft are equal to zero during unaccelerated flight.

The static stability of an aircraft in equilibrium is related to the response of the aircraft to a small disturbance from that equilibrium. If the aircraft initially in static equilibrium state returns to equilibrium after a small disturbance, the state is a stable equilibrium. However, if the aircraft diverges from equilibrium after being slightly disturbed, the state is an unstable equilibrium. In addition, neutral stability is defined as a dividing line between stable equilibrium and unstable equilibrium.

If an aircraft is statically stable in pitch, a negative (nose-down) pitching moment about center of gravity must be produced after a small increase in angle of attack to decrease the angle of attack. Conversely, a small decrease in angle of attack must result in a positive (nose-up) pitching moment to increase the angle of attack. Therefore, it can be concluded that the pitching moment about center of gravity must change with angle of attack such that a restoring moment results.

The general longitudinal static stability criterion for an aircraft can be defined as:

$$\frac{\partial C_{m_{AC}}}{\partial \alpha} \equiv C_{m,\alpha} < 0 \tag{1}$$

Each component of an aircraft has a different effect on the longitudinal stability as shown in Figure 1. Both the wing and fuselage provide a destabilizing nose-up moment when their angle of attack is increased, whereas the horizontal tail alone provides a stabilizing nose-down moment. Thus, a complete aircraft has a stable configuration when wing, body and horizontal tail are brought together.

The horizontal tail is not a necessity for the stability of an aircraft. The center of gravity (CG) has a vital effect on longitudinal stability. Figure 2 shows the variation of pitching moment with angle of attack for different CG positions. The slope of CM/CL line decreases as CG goes to backward up to a point where CM-pitching moment does not change with CL. This point is defined as neutral position which gives neutral stability.
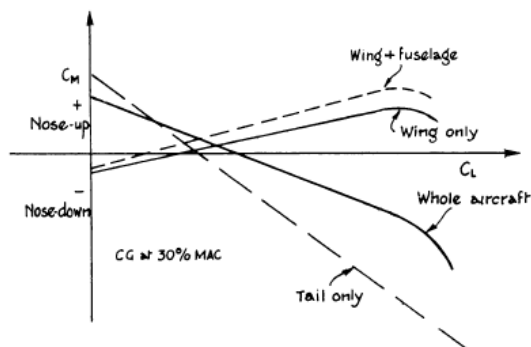
Figure 1: Contribution of each aircraft component on the longitudinal static stability [1]
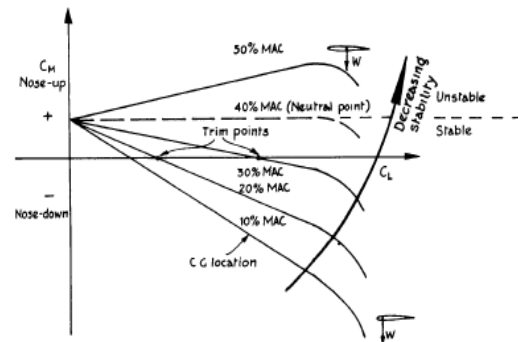
Figure 2: Effect of center-of-gravity on longitudinal static stability [1]

For a conventional aircraft, use of the overall aircraft AC is more useful. Since $C_{m_{AC}}$ does not change with amgle of attack, C_{m_α} can be expressed as:

$$M_{CG} = L(X_{cg} - X_{AC}) + M_{AC} \tag{2}$$

$$C_{m_{cg}} = C_L(X_{cg} - X_{AC}) + C_{m_{AC}} \tag{3}$$

$$C_{m_\alpha} = C_{L_\alpha}(X_{cg} - X_{AC}) \tag{4}$$

If $\bar{X}_{cg}$ is equal to $\bar{X}_{AC}$, C_{m_α} becomes zero. A point about which the total pitching moment does not change with small variations in angle of attack exists on the aircraft. This is like the aerodynamic center of an airfoil or wing. The aircraft is longitudinally stable if the CG is located ahead of this point. This point is commonly called as the stick-fixed neutral point (NP). The stick-fixed neutral point is the aerodynamic center of the whole aircraft. The condition for neutral static stability is significant since it is the boundary between static stability and instability. The NP of the aircraft can be stated as:

$$\bar{X}_{AC} = \bar{X}_{cg} \tag{5}$$

As long as the CG is positioned at the rear of the NP, the aircraft will become longitudinally unstable.

Static margin is another concept to express the level of the longitudinal static stability. Static Margin (SM) can be defined as:

$$SM = \bar{X}_{AC} - \bar{X}_{cg} = -(\bar{X}_{cg} - \bar{X}_{AC}) = \bar{X}_{NP} - \bar{X}_{cg} \tag{6}$$

The static margin is a non-dimensional distance between the NP and the longitudinal CG position. A positive static margin leads to positive longitudinal stability, while a negative static margin leads to negative longitudinal static stability.

Determination of Neutral Point

The neutral point is determined by utilizing the variation of pitching moment coefficient (C_m) with AoA (α). The CG position at which the slope of C_m vs α graph is equal to zero is specified as neutral point.

Neutral points were computed at all specified airspeeds for each of the six horizontal tails. The graph of C_m vs α at 0.2 Mach for HT # 5 is presented in Figure 3 for three CG positions as an example. The slope of the variation of C_m vs α becomes zero at 40 % of MAC, which is specified as the neutral point for this flight condition.
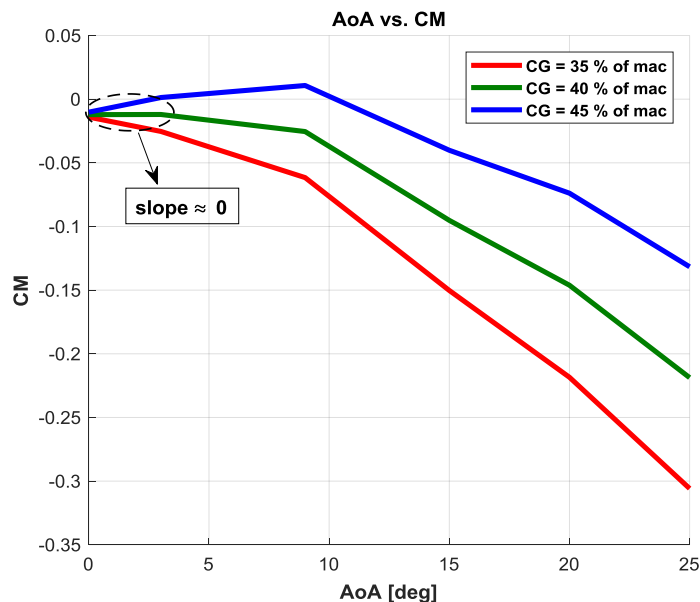
Figure 3: The variation of. Cm with AoA at 0.2 Mach for HT # 5

The neutral points obtained from CFD Analyses are presented in Table 4 for three air speeds. As seen from Table 4, the location of neutral point move rearward substantially throughout subsonic to supersonic regime. In addition, for the results of Datcom analyses, the neutral point slightly move to backward as the horizontal tail volume is increased. However, for the results of CFD analyses, the neutral point shifts towards back in an anticipated level with increase in tail volume.

Sinem Karatoprak, Serkan Özgen

Table 4: The Neutral Points at 0.2, 0.9, and 1.2 Mach Numbers for All Horizontal Tails

Horizontal Tail Number	Neutral Point (% of mac)			
	Subsonic Speed (0.2 Mach)		Transonic Speed (0.9 Mach)	Supersonic Speed (1.2 Mach)
	DATCOM	CFD	CFD	CFD
1	32.5	30	36	56
2	33	31	36.5	57.5
3	35	34	37.5	61
4	36	37	39	64
5	37	40	40	68
6	38	44	42	71

A static margin of at least +5 % is generally a rule of thumb for a conventional aircraft to provide good handling qualities for pilots [2]. However, by utilizing from the relaxed static stability concept, the static margin can be decreased to -7/-10 % [3]. In this study, the most aft CG positions are determined by taking the static margin as -7 % which is a typical value for artificially stable aircrafts.

The most aft CG positions determined from CFD analyses results for both natural and artificial longitudinal stability conditions are presented at below tables.

Table 5: The Most Aft CG Positions in case of Natural Longitudinal Static Stability

Horizontal Tail Number	Most Aft CG Positions for SM = +5 %			
	Subsonic Speed (0.2 Mach)		Transonic Speed (0.9 Mach)	Supersonic Speed (1.2 Mach)
	DATCOM	CFD	CFD	CFD
1	27.5	25.0	31.0	51.0
2	28.0	26.0	31.5	52.5
3	30.0	29.0	32.5	56.0
4	31.0	32.0	34.0	59.0
5	32.0	35.0	35.0	63.0
6	33.0	39.0	37.0	66.0

Table 6: The Most Aft CG Positions in case of Artificial Longitudinal Static Stability

Horizontal Tail Number	Most Aft CG Positions for SM = -7 %			
	Subsonic Speed (0.2 Mach)		Transonic Speed (0.9 Mach)	Supersonic Speed (1.2 Mach)
	DATCOM	CFD	CFD	CFD
1	39.5	37.0	43.0	63.0
2	40.0	38.0	43.5	64.5
3	42.0	41.0	44.5	68.0
4	43.0	44.0	46.0	71.0
5	44.0	47.0	47.0	75.0
6	45.0	51.0	49.0	78.0

When the most aft CG positions for natural and artificial stabilities are compared, it can be clearly seen that the limit of aft CG position can be moved significantly backward with the concept of relaxed static stability.

4.2 Nose-Down Recovery

Maneuverable aircraft can attain very high angles of attack due to low or even negative static longitudinal stability. After the aircraft starts to pitch-up with the application of nose-up control, unstable or nose-up pitching moments also accompany to it. A nose-down pitching moment is required for recovery to overcome the unstable nose-up pitching moment.

A criterion for the required nose-down pitching moment for recovery was determined from the related simulation studies and practical fighter design. A pitching acceleration of 0.3 rad/sec was found to be sufficient by providing a margin for inertial coupling [4].

High angle of attack nose-down pitch control capability is very significant for relaxed static stable aircraft [5]. The level of high angle-of-attack nose-down control authority is determined by five primary factors which are listed as deep stall trim, time required to recover to low angles of attack, inertia coupling, aerodynamic coupling and kinematic coupling [5].

A preliminary indication of nose-down control requirements were developed for RSS aircraft by utilizing the existing knowledge and experience on high angle of attack flight dynamics.

The developed methodology shown in Figure 4 is based on the following relationship:

$$C_m^* = \frac{I_{yy}\dot{q}}{\bar{q}S\bar{c}} = \left(\frac{\dot{q}}{\bar{q}}\right)\left(\frac{I_{yy}}{S\bar{c}}\right) \tag{7}$$
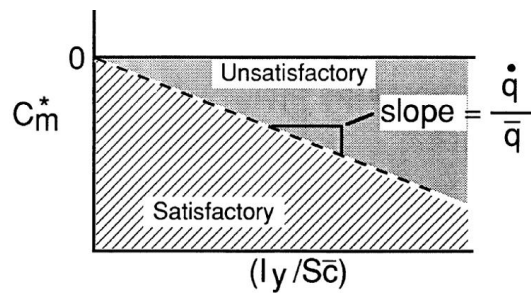
Figure 4: The developed methodology for high AoA nose-down pitch control

The terms in Eq. (7) can be briefly explained as follows:

- The $\left(\frac{\dot{q}}{\bar{q}}\right)$ term can be considered as a response capability stated as pitch acceleration at a specified dynamic pressure.

- The $\left(\frac{I_y}{S\bar{c}}\right)$ term depends only on the mass and geometry characteristics of an aircraft. Therefore, the variation of C_m^* with $\left(\frac{I_y}{S\bar{c}}\right)$ is linear and has a slope equal to $\left(\frac{\dot{q}}{\bar{q}}\right)$ as indicated in Figure 3. An Aircraft with a value on the line will have minimum nose-down pitch control capability, while aircraft having values above the line will have less capability. Aircrafts with values below the line will have greater capability. Therefore, the appropriate slope of C_m^* versus $\left(\frac{I_y}{S\bar{c}}\right)$ should be determined to achieve "satisfactory" high AoA nose-down control capability. In other words, the line shows a "satisfactory" control margin at the point where the nose-down capability is minimum. Based on the studies mentioned in [5], a guideline would be developed. Guideline defines a plot of C_m^* versus $I_y/S\bar{c}$ in which all points falling below the line $C_m^* = -0.006\left(I_y/S\bar{c}\right)$ are considered as "satisfactory" and all points above this line are "unsatisfactory", as shown in Figure 4.

As mentioned earlier, the ratio of $\frac{\dot{q}}{\bar{q}}$ is equal to the slope of the C_m^* versus $I_y/S\bar{c}$; therefore, it can be written as

$$\frac{\dot{q}_{required}}{\bar{q}_s} = -0.006 \tag{8}$$

Sinem Karatoprak, Serkan Özgen

$$\dot{q}_{required} = -0.006\bar{q} \tag{9}$$

A value of $\bar{q}_s$ is typically equal to 40 lb/ft² for current fighter aircraft [4]. Thus,

$$\dot{q}_{required} = -0.24 \text{ rad}/sec^2 \tag{10}$$

Therefore, the minimum required nose-down angular acceleration capability at stall speed and aft CG should be

$$|\dot{q}| \geq 0.24 \ rad/sec^2 \tag{11}$$

which also satisfies the requirement mentioned in [4].

Determination of Aft CG Limit regarding Nose-Down Recovery Capability

The values of $\frac{\dot{q}}{\bar{q}}$ is calculated over a CG range at 0.2 Mach for all horizontal tails. The CG position where the slope of C_m^* versus $I_y/S\bar{c}$ neutral point is equal to zero is determined. This point is the most aft CG at which the required minimum nose down capability exists.

The plot of $\dot{q}/\bar{q}$ vs. CG Position at 0.2 Mach for HT # 5 is presented in Figure 5 as an example. The value of $\dot{q}/\bar{q}$ becomes -0.006 approximately at 63.7 % of MAC which is the most aft CG position regarding minimum nose-down capability.
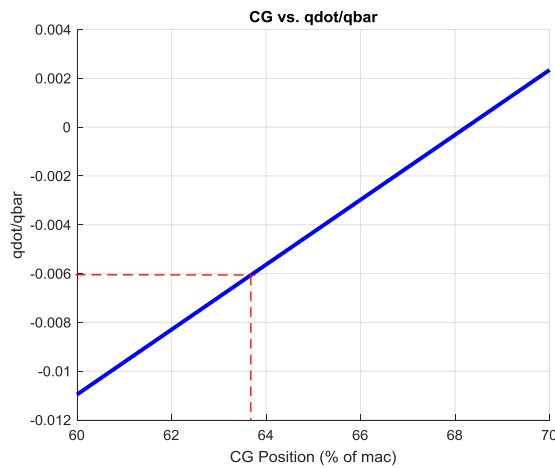
Figure 5: Nose-Down Recovery Characteristic at 0.2 Mach for HT # 5

The CFD Analyses results for nose-down capability characteristics are presented at Table 7 for all horizontal tails.

Table 7: The most aft CG positions regarding the minimum nose-down capability for all horizontal tails

Horizontal Tail Number	$\dot{q}/\bar{q}$	$\dot{q}$ (rad/sec²)(2)	CG Position (% of mac)	
			DATCOM	CFD
1			41	39.0
2			43	42.5
3	-0.006	-0.24	46.5	49.3
4			50	56.4
5			53	63.7
6			56.5	70.9

4.3 Take-Off Rotation

The horizontal tail size required during the take-off rotation is a critical requirement, which sizes the horizontal tail. Most of the aircraft must be rotated about the main landing gear to be able to reach the required angle of attack for lift-off. During the take-off, aircraft normally rotate at low speeds, which are slightly higher than the stall speed. The low dynamic pressures at low speeds decrease the effectiveness of horizontal tail. Therefore, a significant download on the horizontal tail is required for the necessary lift-off capability [6].

Figure 6 indicates the major forces and moments which act on the aircraft during the take-off rotation. The forces on the aircraft during the take-off rotation can be listed as wing lift, horizontal control surface lift, wing-body pitching moment, aircraft drag, aircraft weight, and engine thrust. The acceleration of aircraft is also included. The aircraft rotates about the point of ground contact during take-off rotation. Therefore, the moment arms of each force and moments are taken with respect to their positions from the point of ground of contact. The wing lift is located at the wing aerodynamic center. The drag and acceleration of the aircraft are positioned along the aircraft. The lift of the horizontal tail is placed at its aerodynamic center. The takeoff weight is positioned at the center of gravity. The wing-body pitching moment is placed about the point of contact. A standard take-off procedure is applied during the take-off analysis. This implies that the thrust vector points in the forward direction. Thus, the only moments produced by the thrust vector is owing to the vertical displacement (Z_{T_g}) of the vector.

The following three equations [6] describe the aircraft equilibrium at the instant of take-off rotation:

$$T - D_g - \mu_g R_g = \frac{W}{g}\dot{U} \tag{12}$$

$$L_{wf_g} + L_{h_g} + R_g = W \tag{13}$$

$$-W\left(X_{mg_g} - X_{cg_g}\right) + D_g\left(Z_{D_g} - Z_{mg_g}\right) - T\left(Z_{T_g} - Z_{mg_g}\right) + L_{wf_g}\left(X_{mg_g} - X_{ac_{wf_g}}\right) + M_{ac_{wf_g}} -$$
$$L_{h_g}\left(X_{ac_{h_g}} - X_{mg_g}\right) + \frac{W}{g}\dot{U}\left(Z_{cg_g} - Z_{mg_g}\right) = I_{yy_{mg}}\ddot{\theta}_{mg} \tag{14}$$
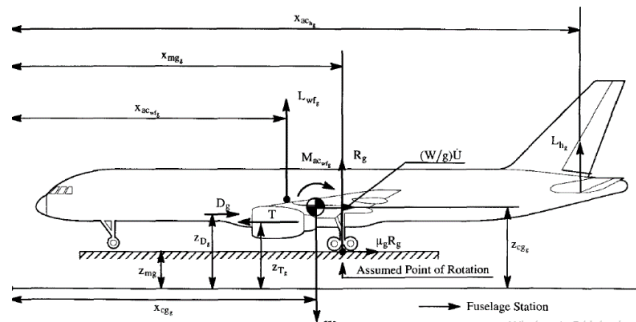
Figure 6: The major forces and moments during take-off [6]

The subscript g associated with most terms in Eqs (12), (13), and (14) represent the ground effect. All forces and moments in *Figure 6* must be evaluated by including the ground effect. μ_g is the wheel-to-ground friction coefficient.

The values of friction coefficient for different ground conditions are taken as 0.02 for concrete or asphalt [6].

The duration of take-off rotation does not exceed 1-3 seconds. Therefore, the angular acceleration about the main landing gear rotation point, $\ddot{\theta}_{mg}$, should be approximately taken between 10-12 deg/sec² for fighters in a preliminary design [6].

The aircraft rotation speed may be related with the stall speed in the take-off configuration during preliminary design [6]:

$$V_{rotate} = V_R \geq 1.1 V_{S_{takeoff}} \tag{15}$$

Determination of Forward CG Limit regarding Take-Off Rotation

The FWD CG limit for take-off rotation at the rotation speed can be solved from Eqns. (12)-(14). The final equation is summarized as:

Sinem Karatoprak, Serkan Özgen

$$X_{cg} = \frac{\begin{bmatrix} I_{yy_{mg}}\ddot{\theta}_{mg} + WX_{\text{mg}} - D(Z_{\text{D}} - Z_{\text{mg}}) + T(Z_{\text{T}} - Z_{\text{mg}}) - L_{wf_g}\left(X_{\text{mg}} - X_{ac_{\text{wf}}}\right) - M_{ac_{\text{wf}}} \\ + L_h\left(X_{ac_h} - X_{mg}\right) - \left\{\left(T - D_g - \mu_g(W - L_{wf} - L_h)\right)(Z_{cg} - Z_{mg})\right\} \end{bmatrix}}{\text{W}} \tag{16}$$

Datcom analyses are performed with/out ground effect. The results illustrate that the ground effect does not cause any difference on the aerodynamic coefficient at this analyses condition. Therefore, the ground effect is not also included to CFD analyses. Therefore, the terms in Eq. (16) are expressed without the subscript g.

Eq. (16) is solved for six horizontal tails by using aircraft specifications listed in Table 1. Required CG positions are obtained such that they can be specified as the FWD CG limits. Table 8 illustrates that the position of FWD CG limit is moved forward as tail volume is increased.

Table 8: Take-Off Rotation Forward CG Limit

Horizontal Tail Number	CG Position (% of MAC)	
	DATCOM Results	CFD Results
1	21	26.5
2	20	25
3	17.5	21.5
4	15.5	18
5	13	13.5
6	11	9

5. Horizontal Tail Sizing Diagram

A typical tail sizing diagram are used to find the minimum required horizontal tail size for the aircraft to meet center-of-gravity requirements. This diagram is known as an x-plot or scissor-plot. In this diagram, the forward and aft center-of-gravity limits are plotted against the non-dimensional horizontal tail volume, which is proportional to the size and moment arm of the horizontal tail. To find the minimum tail size, the smallest value of tail volume is picked for which the distance between the forward and aft limits is equal to the required cg range.

The horizontal tail location is determined by the moment arm. The moment arm is the distance between the positions of the neutral points of the wing and horizontal tail. The area ratio S_H/S_{ref} and the relative tail distance $l_{HT}/\bar{c}$ are significant characteristic ratios of the horizontal tail. These dictate the size and position of the horizontal tail in relation to the wing. The product of these two ratios gives the tail volume ratio which can be defined as

$$C_{HT} = \frac{l_{HT}S_{HT}}{\bar{c}\,S_{ref}} \;[7] \tag{17}$$

The horizontal tail sizing diagrams for each of the horizontal tails are obtained for both natural and artificial stability conditions including CFD and Datcom based analyses results as indicated from Figure 7 to Figure 30. The solid blue lines illustrate take-off rotation and stability CG limits, respectively while the dash blue line shows the nose-down control CG limit. The black line indicates the allowable CG range between the FWD and aft CG limits.

The FWD CG limit is determined from the required CG during take-off rotation while the aft CG limit is determined from the level of minimum required stability. The aft CG limit can be extended by utilizing from the concept of RSS. This causes extension of the allowable CG range which can be clearly seen from Figure 7 and Figure 8.

The allowable CG range also increases with increase in tail volume ratio (C_{HT}) for both natural and artificial stability conditions as seen from tail sizing diagrams.

The tail sizing diagrams obtained from CFD results are presented below.
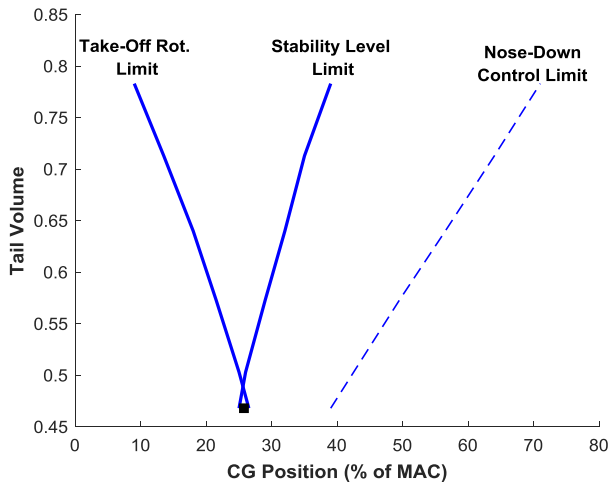
Figure 7: Tail Sizing Diagram of HT#1 for Natural Stability
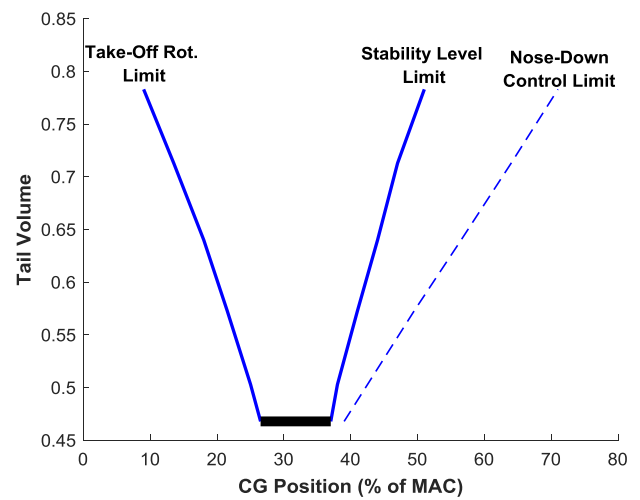
Figure 8: Tail Sizing Diagram of HT#1 for Artificial Stability
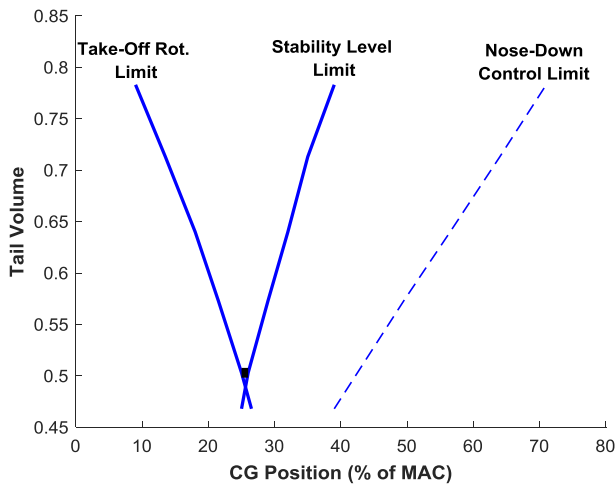
Figure 9: Tail Sizing Diagram of HT#2 for Natural Stability
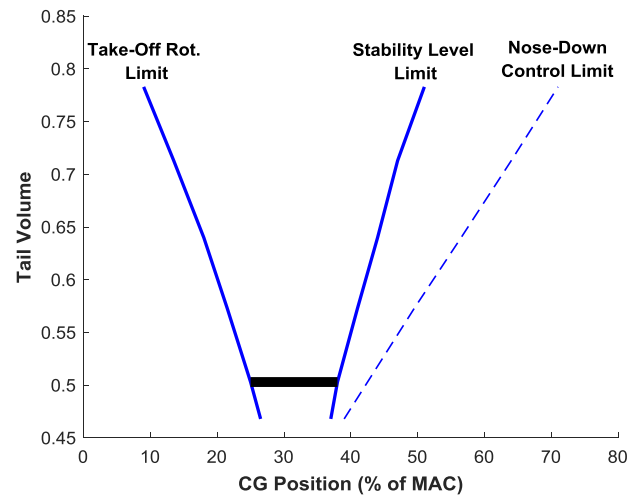
Figure 10: Tail Sizing Diagram of HT#2 for Artificial Stability
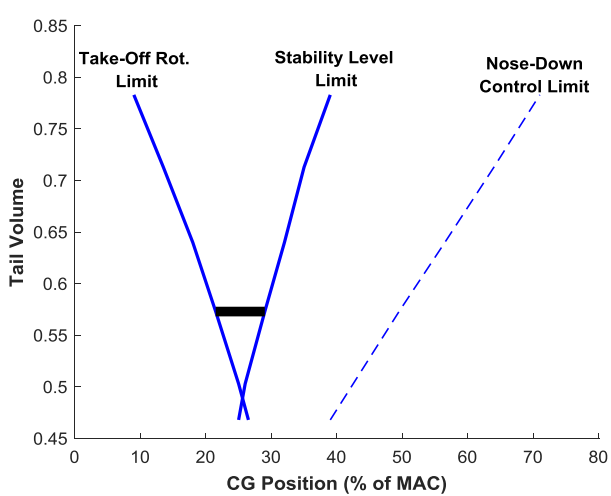
Figure 11: Tail Sizing Diagram of HT#3 for Natural Stability
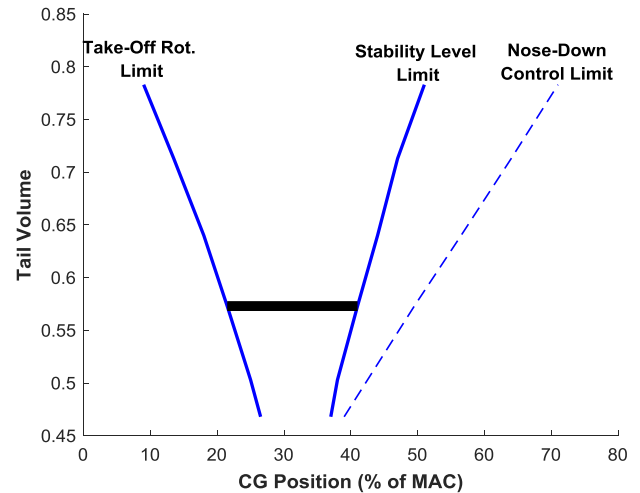
Figure 12: Tail Sizing Diagram of HT#3 for Artificial Stability
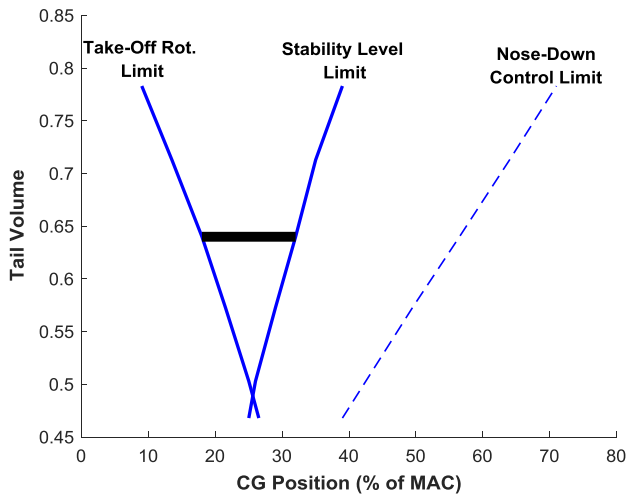
Figure 13: Tail Sizing Diagram of HT#4 for Natural Stability
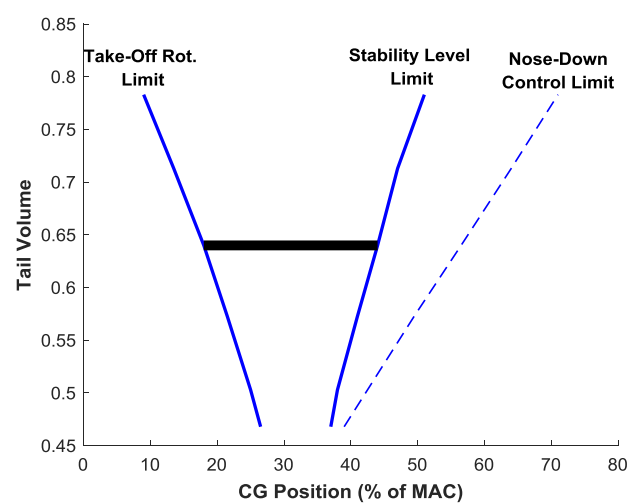
Figure 14: Tail Sizing Diagram of HT#4 for Artificial Stability
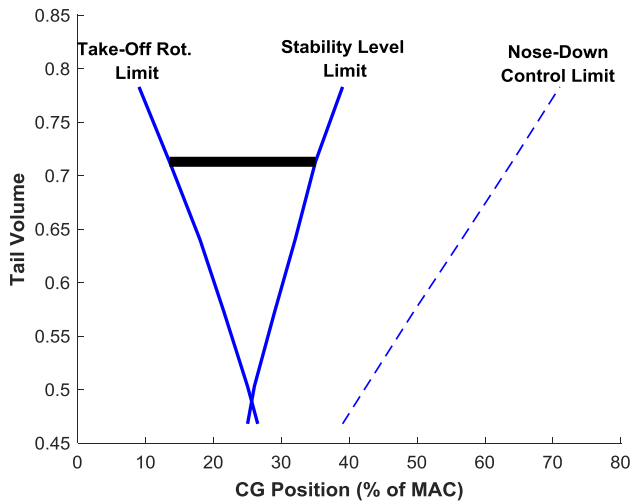
Figure 15: Tail Sizing Diagram of HT#5 for Natural Stability
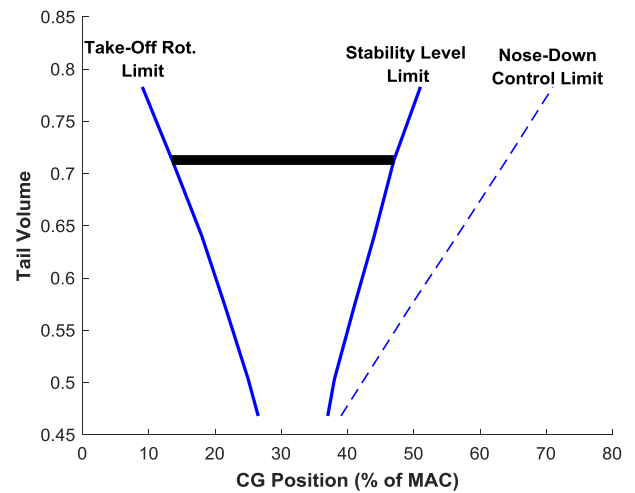
Figure 16: Tail Sizing Diagram of HT#5 for Artificial Stability
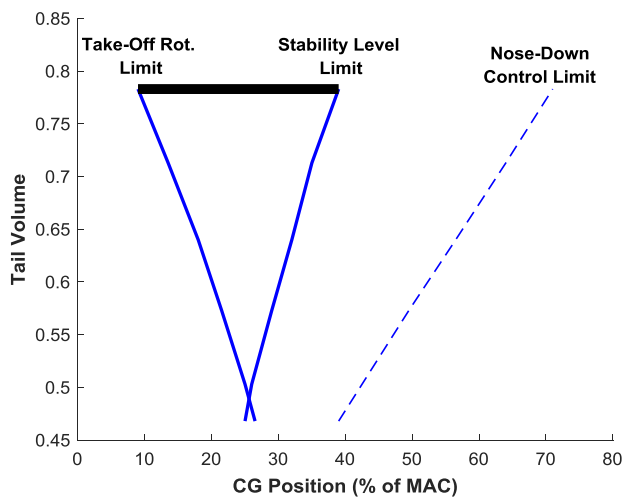
Figure 17: Tail Sizing Diagram of HT#6 for Natural Stability
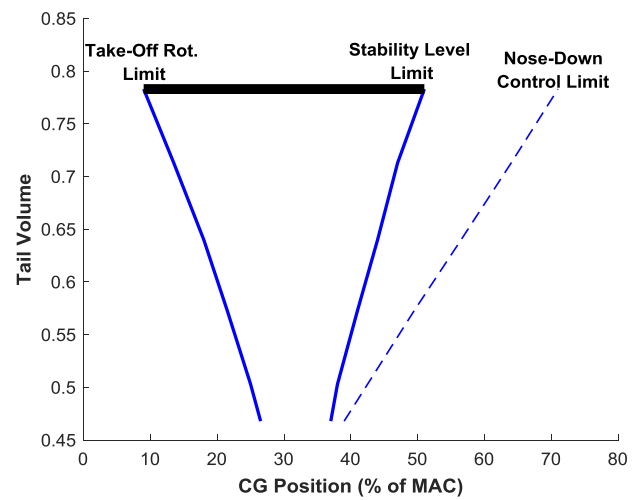
Figure 18: Tail Sizing Diagram of HT#6 for Artificial Stability

The tail sizing diagrams obtained from Datcom results are presented below.
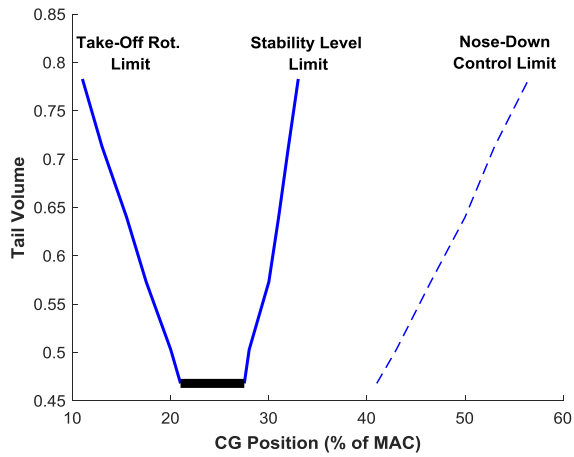
Figure 19: Tail Sizing Diagram of HT#1 for Natural Stability
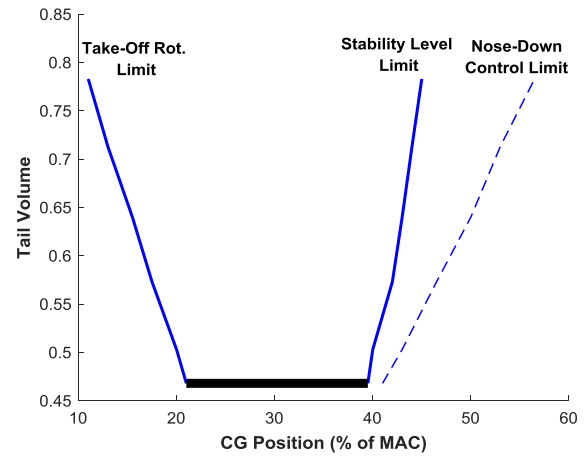
Figure 20: Tail Sizing Diagram of HT#1 for Artificial Stability
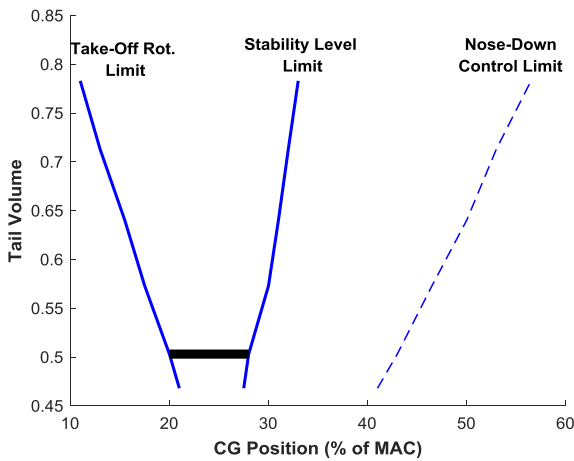
Figure 21: Tail Sizing Diagram of HT#2 for Natural Stability
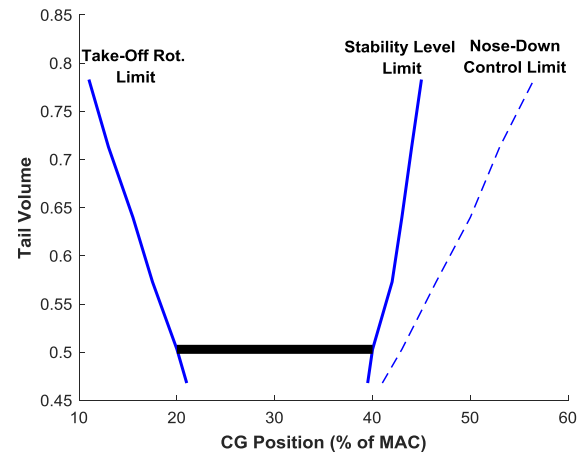
Figure 22: Tail Sizing Diagram of HT#2 for Artificial Stability
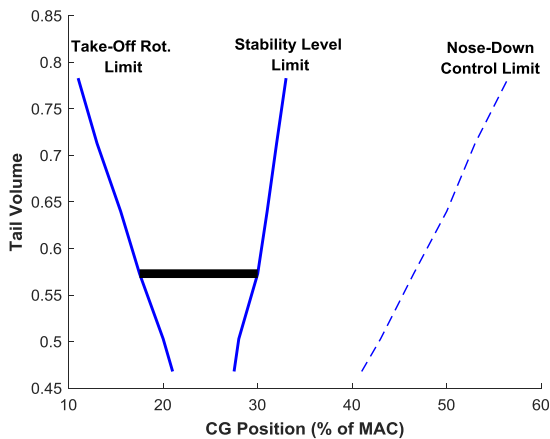
Figure 23: Tail Sizing Diagram of HT#3 for Natural Stability
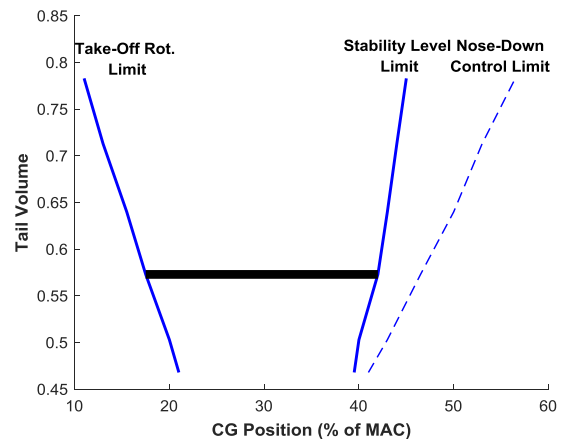
Figure 24: Tail Sizing Diagram of HT#3 for Artificial Stability
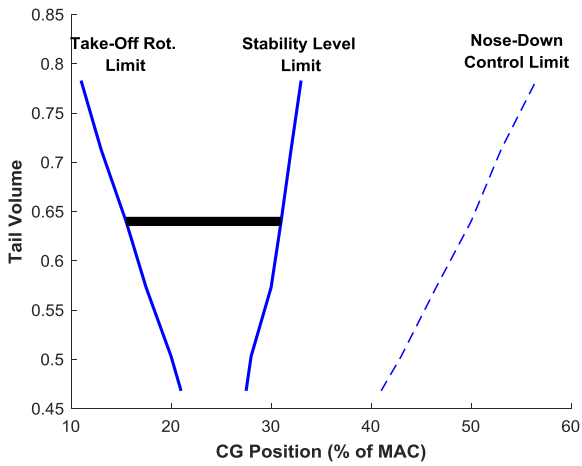
Figure 25: Tail Sizing Diagram of HT#4 for Natural Stability
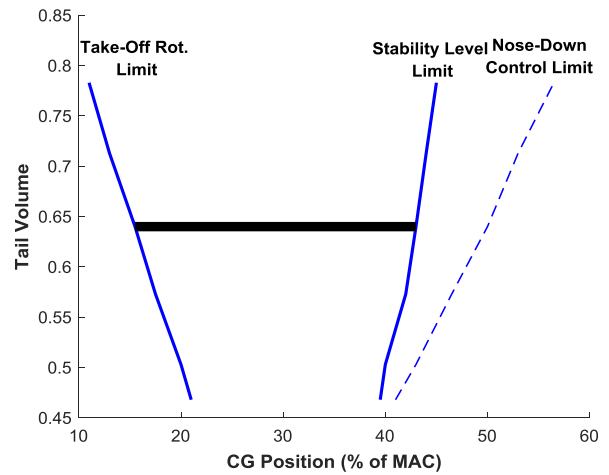
Figure 26: Tail Sizing Diagram of HT#4 for Artificial Stability
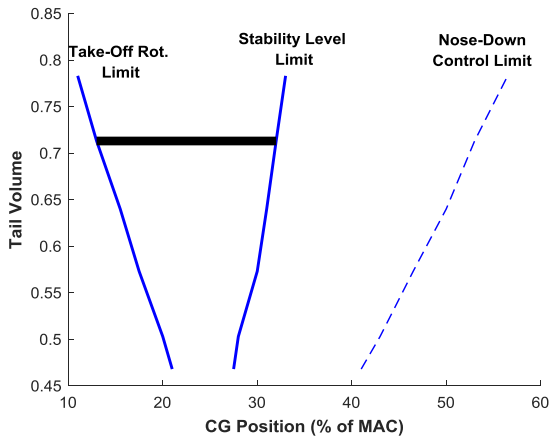
Figure 27: Tail Sizing Diagram of HT#5 for Natural Stability
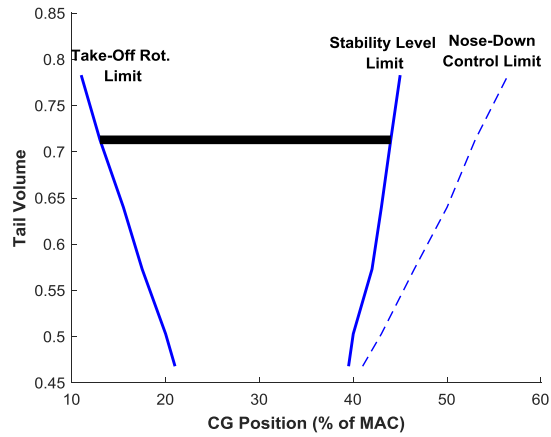
Figure 28: Tail Sizing Diagram of HT#5 for Artificial Stability
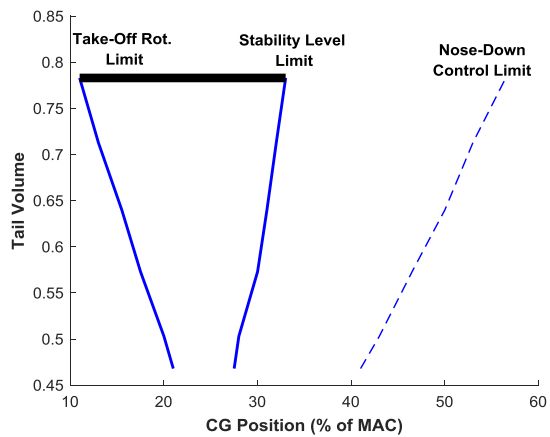
Figure 29: Tail Sizing Diagram of HT#6 for Natural Stability
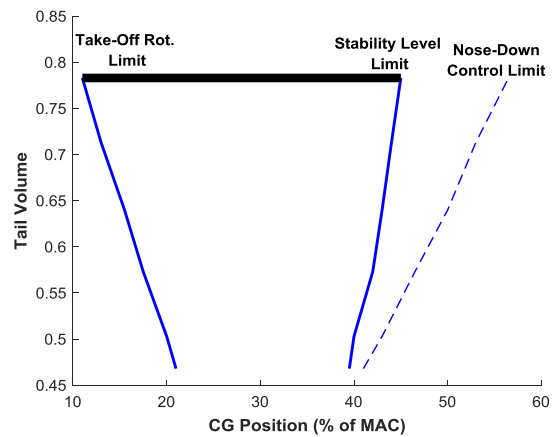
Figure 30: Tail Sizing Diagram of HT#6 for Artificial Stability

7. Conclusion

In this study, the tail sizing diagrams are generated for six different horizontal tail planforms of a conventional jet trainer aircraft.

The FWD CG limit is determined from the most FWD CG position required to lift the nose up during the take-off rotation. The horizontal tail must have necessary control capability at FWD CG position. The most FWD CG position is calculated from Eq. (16) by utilizing from some major aircraft specifications listed in Table 1.

The aft CG limit is determined from either the minimum required level of static stability or nose-down recovery capabilityat high AoAs. The level of static stability is obtained from the static margin. The static margin must be at least +5 percent for natural stability condition [2]. When the static stability is relaxed, the static margin can be decreased up to -7 percent [3]. The values of static margin are calculated for both natural and artificial stability conditions for six horizontal tails. The aft CG limit is also determined from the minimum required nose-down capability at high AoA. The most aft CG positions for minimum nose-down pitch control capability are computed by utilizing from the guideline mentioned in Section 4.2 [5] for six horizontal tails. The results of the analyses indicate that the necessary level of stability is more critical than the minimum nose-down capability for the determination of the aft CG limit. Therefore, the level of static stability of the aircraft determines the aft CG limit.

The tail sizing diagrams are created from the results based on both CFD and DATCOM analyses for natural and artificial stability conditions. The CG limits are specified in the tail sizing diagrams. The allowable CG range between these CG limits are also indicated in the diagrams.

When the operational CG range specified between 35 % and 39% of MACs (Table 1) is considered, the following comments can be done.

For the results based on CFD analyses:
- The limit of FWD CG position can be met for six horizontal tail planforms.
- The limit of aft CG position can be satisfied with only HT # 6 for natural stability condition while this limit can be satisfied with HT # 3, HT # 4, HT # 5 and HT # 6 for artificial stability condition.

For the results based on Datcom analyses:
- The limit of FWD CG position can be satisfied for six horizontal tail planforms.
- The limit of aft CG position cannot be fulfilled any horizontal tail planform for natural stability condition. However, when the static stability is relaxed, the aft CG limit can be met for six horizontal tail planforms.

As a result of these studies, by considering the most critical results obtained from CFD analyses, it can be concluded that the horizontal tail planform can be reduced from 12.2 m^2 (HT # 6) to 8.9 m^2 (HT # 3) with the concept of relaxed static stability. This reduction in horizontal tail, surely, causes a decrease in aircraft weight, a decrease in trim drag, and thus an increase in maneuverability.

References

[1] R. Whitford. 1987. Design for Air Combat.Jane's Publishing. 162-179.

[2] W. F. Phillips. 2010. Mechanics of Flight. John Wiley & Sons, Inc. 381-421.

[3] D. C. Aronstein and A. C. Piccirillo. 1996. The Lightweight Fighter Program: A Successful Approach to Fighter Technology Transition. AIAA Education. 21.

[4] M. J. Abzug and E. E. Larrabee. 2002. Airplane Stability and Control, A History of Technologies That Made Aviation Possible. Cambridge University Press.161.

[5] L. N. Nguyen and J. V. Foster. 1990. Development of a Preliminary High-Angle-of-Attack Nose-Down Pitch Control Requirement for High-Performance Aircraft. NASA Technical Memorandum 101684. National Aeronautics and Space Administration.

[6] J. Roskam. 2001. Airplane Flight Dynamics and Automatic Flight Controls. DARcorporation. 288-291.

[7] L. M. Nicolai, G. E. Carichner. 2010. Fundamentals of Aiircraft and Airship Design Volume 1-Aircraft Design. AIAA Education. 289.

[8] R.D. Finck. 1978. USAF Stability and Control DATCOM, AFWAL-TR-83-3048. Wright-Patterson Air Force Base. McDonnell Douglas Corporation.